JOURNAL OF PROPULSION AND POWER
Vol. 23, No. 4, July–August 2007

Performance and Active Thermal Control of 2-kW Hall Thruster with Segmented Electrodes

Alex Kieckhafer,* Dean Massey,* and Lyon B. King†
Michigan Technological University, Houghton, Michigan 49931

DOI: 10.2514/1.21820

The performance and plume characteristics of a 2-kW Hall thruster with segmented anodes for thermal control of the main anode are characterized. Diagnostics performed included thrust, specific impulse, and efficiency, as well as the ion current density in the plume. The apparatus included an inverted-pendulum thrust stand for performance measurements and a shielded Faraday probe for ion current density characterization. Data were taken at several operating points and at several ratios of current to the main anode vs the shim electrodes. The data show a general increase in centerline current density, thrust, specific impulse, and efficiency as discharge current is moved to the shims. Thermal measurements show up to 50°C control authority in the main anode temperature.

Nomenclature

$\langle E \rangle$ = average ion energy
J_i = ion current density
J_m = measured ion current density
γ = secondary electron yield

I. Introduction

CURRENT flight Hall thrusters use xenon gas as a propellant. Although xenon is effective, it may not be ideal for future high-power devices because of a number of problems. The first problem is the expense of xenon, making extended testing of large Hall thrusters very costly. Additionally, the operation of a xenon thruster in a vacuum chamber requires very large pump throughput to remove the influx of propellant gas efficiently. One method of potentially reducing the cost of ground operations, while also improving the performance of a Hall thruster, is to use condensable propellants such as bismuth. Bismuth offers two major advantages for ground testing: low propellant cost and its condensable nature. Bismuth is much cheaper than xenon [1]. The large difference in price will allow extended testing programs on large thrusters to cost much less with bismuth than with xenon. The condensable nature of bismuth aids in ground testing as propellant ions will condense on vacuum facility walls, effectively making bismuth "self-pumping." With that in mind, operating a 50-kW bismuth Hall thruster would require only enough pumping speed to keep up with the chamber leaks and cathode mass flow (assuming a xenon cathode). Bismuth also offers several performance advantages over xenon, which increases its attractiveness as a propellant for higher thrust-to-power applications [1].

Although immature as a Hall thruster propellant, the use of bismuth is not without precedent [2]. Soviet work performed in the 1970s and 1980s evaluated bismuth anode-layer thrusters. Central Scientific Research Institute for Machine Building (TsNIIMASH) researchers reported thrusters with a power level up to 140 kW and specific impulse as high as 8000 s at anode efficiencies exceeding 70% [3]. The anode-layer thrusters in these studies differ from the stationary plasma thruster (SPT)-type studied here in that the discharge channel of an anode-layer thruster is shallow and the walls are also the anode surface. SPT-type thrusters use an anode at the base of a deeper channel than anode-layer thrusters, with the channel walls made of ceramic material. More recently, efforts under the Very High Impulse Thruster with an Anode Layer Program have made progress toward development of a very high specific impulse, high-power thruster.

Bismuth presents its own engineering difficulties, however. For the thruster to operate, there must be a precisely controlled source of bismuth vapor. Previous work used a heated bismuth reservoir that fed vapor directly into the thruster. The difficulty with this method was that the reservoir required significant resistive heating to maintain a temperature high enough to vaporize bismuth in sufficient quantities (more than 1000 K), as the vapor pressure of bismuth is the driving factor in the evaporation rate and is dependent on temperature. To reduce or eliminate the need for resistive heating, the authors have developed a technique that uses the waste heat from the thruster to warm the bismuth reservoir to the required temperatures. In this design, the main anode of the thruster functions as the bismuth reservoir. As the anode is heated by the thruster discharge plasma, this design has the potential to eliminate the need for resistive heaters during operation. This approach will allow the anode to be maintained at a temperature sufficient for bismuth evaporation purely from the discharge waste heat. The evaporation rate is controlled through the reservoir temperature and the permeated area through which the bismuth vapor diffuses into the discharge chamber. Because it is not practical to vary the vapor escape area through the reservoir mechanically, the mass flow rate $\dot{m}$ is controlled by varying the reservoir temperature within the thruster. The evaporation rate is governed by the equilibrium vapor pressure of the liquid metal with the resultant goal of maintaining the appropriate evaporator temperature, which when combined with the open area produces sufficient quantities of bismuth vapor. Previous studies have found that for an anode with a 10% open-area fraction in a thruster of the type investigated in this paper, a temperature of 750°C is sufficient to provide the necessary bismuth mass flow (5–6 mg/s in the examined thruster) [4].

Control of the anode/reservoir temperature is necessary to control the flow of bismuth. To control the temperature of the main anode, a pair of inert shim electrodes was added to the discharge channel of the thruster, downstream of the main anode, as shown in Fig. 1. By slightly varying the shim electrode voltage with respect to the main anode/reservoir, the discharge current can be shifted between the shim electrodes and the main anode. This shift in discharge current will then shift the discharge heating, with the result that shifting current to the shims will cool the main anode, while diverting current back to the anode will increase its temperature, and hence the bismuth evaporation rate [5]. The shim electrodes were fabricated

Received 15 December 2005; revision received 8 February 2007; accepted for publication 9 February 2007.

*Ph.D. Candidate, 815 R. L. Smith Building, 1400 Townsend Drive. Student Member AIAA.
†Associate Professor, 815 R. L. Smith Building, 1400 Townsend Drive. Member AIAA.

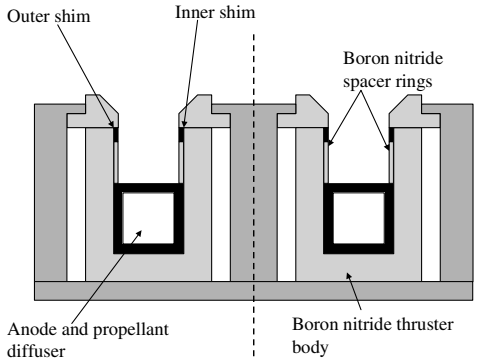

Fig. 1 Cross-sectional view of the thruster with shim electrodes and main anode.

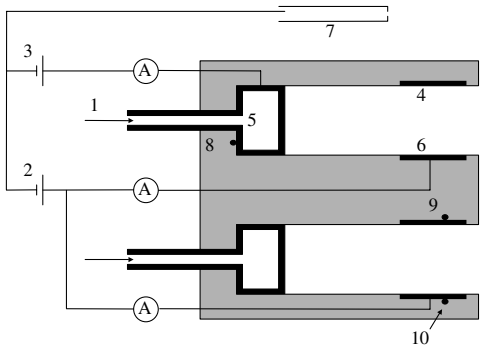

Fig. 2 Electrical schematic of thruster test apparatus. Numbered annotations are 1: xenon propellant flow, 2: shim power supply, 3: main anode power supply, 4: outer shim electrode, 5: main anode and gas distributor, 6: inner shim electrode, 7: cathode, 8: anode thermocouple, 9: inner shim thermocouple, and 10: outer shim thermocouple.

from nonmagnetic stainless steel so as to impact the magnetic field of the thruster as little as possible.

Although the segmented electrodes present a unique thermal control strategy, the nontraditional configuration may cause a change in the operating characteristics of the thruster. Any negative impact on beam divergence, efficiency, specific impulse, or thrust could negate the anticipated performance benefits of the bismuth scheme. One use of segmented electrodes in previous studies was as a method of achieving two-stage operation [6], where the shim electrodes are maintained at a potential between the anode and the cathode, allowing for an acceleration-only stage for high specific impulse operation. Other experimental investigations have been performed on segmented-electrode Hall thrusters and showed a net decrease in beam divergence and an increase in thrust with the addition of the segmented electrodes [7–9]. These investigations were performed on thrusters with very different operating parameters than the design implemented in this paper. In many of the experiments, the shim electrodes were held either at anode potential, cathode potential, or just allowed to float (as opposed to being forced to accept varying fractions of the discharge current). Some of the shim electrode configurations previously investigated were also emissive in nature. Between the differences in materials, thruster operating regime, and the method of power application to the shim electrodes any attempt to predict the behavior of a candidate segmented anode bismuth thruster, particularly at moderate power levels, is necessarily precluded without experimental observation. Previous experiments on a similar thruster design intended for bismuth operation showed little change in the beam profile [10].

II. Goal of Research

The first goal of the research reported here is to determine the effect, if any, the addition of shim electrodes has on the performance of a 2-kW Hall thruster. The second goal is to determine if the required anode temperature of 750°C can be achieved. Additionally, the temperature range of the anode as the discharge current is moved between it and the shim electrodes will be determined. Comparisons were not made between the tested thruster and existing designs.

III. Experimental Apparatus

A. Hall Thruster

The Hall thruster employed by the Ion Space Propulsion Lab at Michigan Technological University for preliminary segmented anode tests uses the magnetic circuit from an Aerojet-constructed BPT-2000 [11] that has been retrofitted with segmented anodes, the necessary power connections as well as instrumentation for temperature measurements. Adjustments of the current-sharing properties of the anodes are accomplished by independently varying the voltages of the shim electrodes as shown in Fig. 2 while keeping the main anode at a fixed potential. The difference between the tested thruster when shim and anode potentials were identical, and the original BPT-2000 is in the location of electrodes. The original thruster used a cup-shaped anode that lined the entire discharge channel. In the tested thruster, with equal potentials on anode and shims there is a boron–nitride spacer inside the channel that is used to separate the shim electrodes from the main anode, and thus will change the nature of the discharge slightly because of the presence of an insulator instead of a conductor in that location. A single cathode is employed as both neutralizer and discharge cathode. Cathode mass flow was maintained at 0.3 mg/s for all testing. Electrical connections to the shim electrodes were made through the use of high temperature wire welded directly to the anode and passed through the boron–nitride thruster body. Thermocouples were connected similarly. The main anode and shim electrodes were constructed from stainless steel.

B. Thruster Testing Facility

All tests were performed in the Ion Space Propulsion Lab's Xenon Test Facility (XTF). The facility is composed of a 2-m-diam by 4-m-long vacuum tank. Rough pumping is accomplished by a two-stage rotary oil-sealed vacuum pump with a Roots blower, capable of pumping at 200 l/s. High vacuum is achieved through dual 48-in.-diam cryopumps, capable of a combined pumping rate of 120,000 l/s on nitrogen as in Fig. 3. Tank pressure was measured via a Bayard-Alpert ionization gauge mounted behind the thruster, on one of the end caps of the tank.

C. Performance Measurements

Thrust measurements were taken using an inverted-pendulum thrust stand [12] and recorded via a computer-controlled data acquisition system. Thrust measurements have an estimated experimental uncertainty of 5%. Thermal measurements of the thruster were taken using K-type thermocouples that were directly welded to the shim electrodes and press fit against the back face of the main anode. Because all thermocouples were at anode potential, temperatures were taken manually through the use of electrically isolated thermocouple monitors at approximately 1 min intervals.

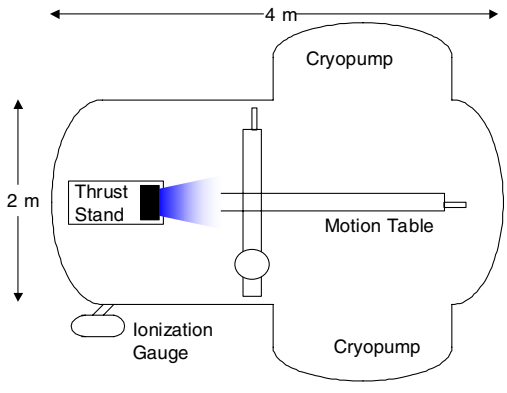

Fig. 3 Diagram of the XTF.

The thermocouple monitors have an uncertainty of 1%. Voltage and current measurements were taken by a computer-controlled data acquisition system that polled the power supplies at approximately 1 s intervals. Uncertainty in the voltage and current measurements was less than 1%.

D. Probe Measurement System

Probe data were taken by use of a 2.4-mm-diam tungsten Faraday probe, as displayed in Fig. 4. The probe was enclosed in an alumina sheath with an outer diameter of 4.75 mm. A steel guard ring with a diameter of 10 mm was included to reduce edge effects on the potential structure in front of the probe face. The probe voltage was chosen based on a current–voltage characteristic of the plasma, using a voltage in the ion saturation regime. Both probe and guard ring were biased 27 V below ground; 1–3 V below the cathode, which was floating between 24 and 26 V below ground during thruster operation. Probe measurements were taken using a high-voltage source meter set for constant voltage output. Voltage was supplied to the guard ring through a dc power supply, operating at the same voltage as the sourcemeter. The probe was swept across the plume at a constant radius from the thruster to the probe tip, using the exit plane of the thruster as the zero point. The centerline of the probe was aligned with the thruster axis at the center point of the probe sweeps. The probe was rotated so as to be pointed toward the thruster axis at the exit plane for all measurements. Motion of the probe was accomplished by use of a motion table capable of two-dimensional horizontal motion as well as rotation about the vertical axis. Sweeps were performed at radii of 250 and 500 mm and swept through 53.1 and 23.6 deg half-angles, respectively, because of tank volume constraints. Each 250-mm-radius sweep consisted of 51 equally spaced points. The 500-mm-radius sweeps consisted of 25 spatial points at the same displacement angles as the 250-mm-radius sweeps. The error in the probe positioning system was approximately 0.5 mm. The expected error in the ion current measurements was less than 1%; duplicate measurements were different by much less than 1%.

Calculating the ion current density from current collected by a Faraday probe requires dividing collected current by the area of the probe, then applying the equation [13]

$$J_i = J_m - \gamma(\langle E \rangle) J_m \tag{1}$$

The choice of tungsten for probe material is useful here, as γ is small for ion energies within the plume. The value of γ chosen was 0.038; this comes from the yield of singly and doubly charged xenon ions under the expected acceleration energies (270 eV for a thruster operating with shims and main anode at 300 V) [14]. This number was determined by multiplying the secondary electron emission coefficient of both singly and doubly charged xenon by their respective abundances, and adding these together. The expected abundances of singly and doubly charged xenon were 90% And 10%, respectively. Ion energies were chosen based on previous experimental results on Hall thrusters, which showed average ion energies slightly below the discharge voltage [15]. This value was used for all Faraday probe data taken of the thruster over the entire range of voltages examined, as the secondary electron emission coefficient is largely constant over the range of voltages examined.

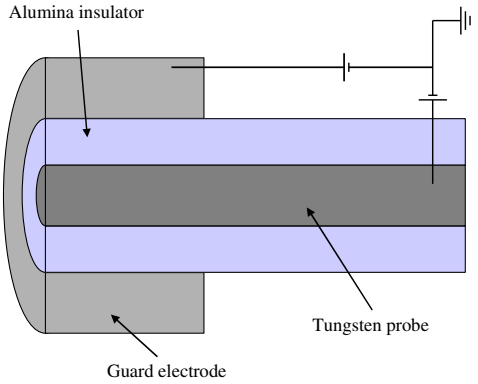

Fig. 4 Cross section of the Faraday probe used.

IV. Experimental Results

The thruster was operated at four different flow rates: 4.0, 5.0, 6.0, and 7.0 mg/s of xenon, and at three main anode voltages: 300, 350, and 400 V. Probe measurements were not taken at 4 mg/s of xenon and thrust measurements were not taken at 7 mg/s. The thruster cathode floated between 24 and 26 V below ground throughout testing. The ability to easily shift and share the total discharge current between shim electrodes and main anodes was confirmed, however, it was discovered that the thruster would not run stably with 100% of the discharge current on the main anode. Attempting to do so (effectively allowing the shims to float) would cause large instabilities or quench the discharge completely. To prevent this, at least 150 mA was maintained on the shims at all times. For probe sweeps, four levels of current sharing were chosen for the nine operating combinations: all current on the shim electrodes, nearly all current on the main anode (except for the 150 mA on the shims), and two equally spaced points where both anode and shim electrodes were receiving different amounts of current. Operating conditions are listed in Table 1. Each condition has been given a label for reference in later sections of this document. At each operating point, the magnetic field was adjusted to minimize the total discharge current when the shim electrode and main anode voltages were equal. This value of magnet current was then sustained as discharge current was shifted from the shim electrode to the main anode by leaving the main anode potential fixed and lowering the shim electrode voltage. In all cases, the shim electrodes never needed to be lowered more then 40 V below the main anode for complete main anode current attachment. During all testing, the tank pressure remained below 2.3×10^{-5} Torr (3.07×10^{-3} Pa) corrected for xenon, as measured by the ionization gauge mounted on the end of the tank, behind the thruster.

A. Performance Data

The general trend in performance as current was shifted from the shims to the main anode was a small reduction in thrust, specific impulse, and efficiency. Figure 5 illustrates a typical case (400 V on the anode, 6.0 mg/s of xenon), and also displays the total discharge current, which remained largely the same as the shim current was adjusted. Figure 6 shows the trends in performance at all operating points. At all voltages and propellant flow rates, the anode efficiency and anode specific impulse decreased as current was diverted from the shim electrodes to the main anode. In some cases, the efficiency decreased by as much as 6%, and the specific impulse was reduced by nearly 100 s.

B. Thermal Data

After completion of performance testing, the variation in anode/shim electrode temperature as a function of current attachment was investigated. To establish the range over which the temperatures could be controlled, the thruster was allowed to come to thermal equilibrium with the current completely attached to each electrode. Figure 7 shows how the thruster responds to both current shifting and mass flow increases with the main anode voltage fixed at 400 V. The main anode temperature varied between approximately 425°C at 5 mg/s with all current on the shim electrodes to nearly 600°C at 7 mg/s with current on the main anode.

C. Faraday Probe Data

The beam profiles showed several differences between shim electrode voltage operating points, as shown in Fig. 8. With the exception of the 305 set of conditions, all operating points showed a significant increase in centerline ion current density when all the current was on the shim electrodes, but very little change between the other three shim electrode voltage levels. In the 357-1 operating condition the peak density increased by nearly a factor of 2 over the

Table 1 Thruster operating conditions: voltages are measured with respect to cathode; cathode flow rate was 0.3 mg/s of xenon

Thruster operating conditions examined						
Anode voltage, V	Shim voltage, V	Anode current, A	Shim current, A	Total current, A	Power, kW	Condition label
			4.0 mg/s			
300	300	0.58	3.14	3.72	1.12	304-1
	293	1.55	2.14	3.69	1.09	304-2
	289	2.15	1.48	3.63	1.07	304-3
	270	3.34	0.15	3.60	1.05	304-4
350	350	0.66	2.98	3.64	1.27	354-1
	344	1.37	2.27	3.64	1.26	354-2
	335	2.49	1.09	3.58	1.24	354-3
	319	3.36	0.16	3.52	1.23	354-4
400	400	0.66	3.02	3.68	1.47	404-1
	391	1.61	2.06	3.67	1.45	404-2
	383	2.60	1.00	3.60	1.42	404-3
	367	3.39	0.15	3.54	1.41	404-4
			5.0 mg/s			
300	300	0.10	4.74	4.84	1.45	305-1
	287	1.59	3.07	4.66	1.36	305-2
	280	3.11	1.49	4.6	1.35	305-3
	266	4.37	0.15	4.52	1.35	305-4
350	350	0.34	4.39	4.73	1.66	355-1
	338	1.73	2.98	4.71	1.62	355-2
	333	3.07	1.57	4.64	1.60	355-3
	314	4.40	0.15	4.55	1.59	355-4
400	400	0.31	4.32	4.63	1.85	405-1
	386	1.82	2.94	4.76	1.87	405-2
	379	3.14	1.55	4.69	1.84	405-3
	360	4.44	0.15	4.59	1.83	405-4
			6.0 mg/s			
300	300	0.50	5.27	5.77	1.75	306-1
	284	2.44	3.57	6.01	1.79	306-2
	279	3.97	1.86	5.83	1.73	306-3
	264	5.55	0.15	5.7	1.70	306-4
350	350	0.28	5.2	5.48	2.02	356-1
	334	2.45	3.54	5.99	2.08	356-2
	328	4.03	1.84	5.87	2.04	356-3
	314	5.65	0.15	5.8	2.02	356-4
400	400	0.33	5.33	5.66	2.34	406-1
	381	2.50	3.55	6.05	2.39	406-2
	377	4.09	1.85	5.94	2.35	406-3
	361	5.73	0.15	5.88	2.35	406-4
			7.0 mg/s			
300	300	0.17	6.55	6.72	2.13	307-1
	282	2.90	4.44	7.34	2.17	307-2
	277	4.91	2.3	7.21	2.13	307-3
	263	7.01	0.15	7.16	2.15	307-4
350	350	0.28	6.4	6.68	2.45	357-1
	330	2.89	4.34	7.23	2.49	357-2
	327	4.98	2.24	7.22	2.50	357-3
	311	7.04	0.15	7.19	2.51	357-4
400	400	0.39	6.37	6.76	2.82	407-1
	382	2.88	4.3	7.18	2.84	407-2
	376	4.94	2.23	7.17	2.84	407-3
	360	6.99	0.15	7.14	2.85	407-4

rest of the 357 group. Operating conditions 356, 357, and 307 also showed significantly lower ion current density at large off-axis angles when the shim electrodes were operating at the same voltage as the anode, in some cases 50% less than the other voltage levels. The operating conditions with reduced shim electrode voltage and current were very similar, differing by only a few percent at maximum.

Measurements of ion current density at 500 mm from the thruster exit plane appear to have many of the same trends as the data at 250 mm, as shown in Fig. 9. Although magnitudes are different, the same increase in peak current density when shim electrode and main anode voltages are equal is still present. The increase is not as drastic, however, with the largest change being an increase of approximately 50%. The reduction in high off-axis current density seen in the 356, 357, and 307 sets of data at 250 mm is not present at 500 mm. The data at 500 mm suggest that the total beam divergence is somewhat larger than that of the original BPT-2000 thruster [11]. This finding could be due to a suboptimal magnetic field, as the field was tuned to minimize discharge current and not to maximum thrust efficiency.

V. Discussion

A. Performance Data

Performance testing demonstrated that operating with segmented anodes alters thruster performance by less than 6%. Shifting current attachment from shim electrodes to the main anode neither affects

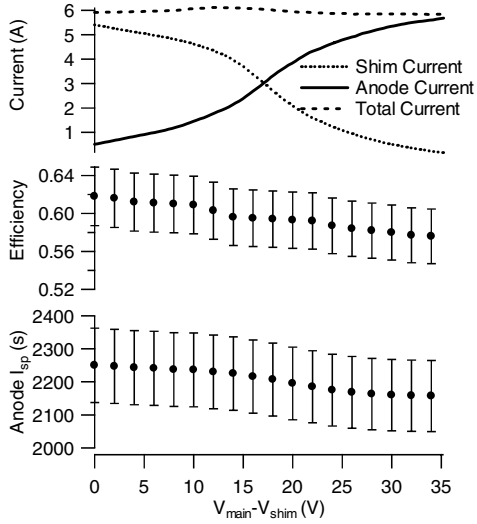

Fig. 5 Current, efficiency, and specific impulse as a function of shim electrode voltage for the 406 set of operating conditions.

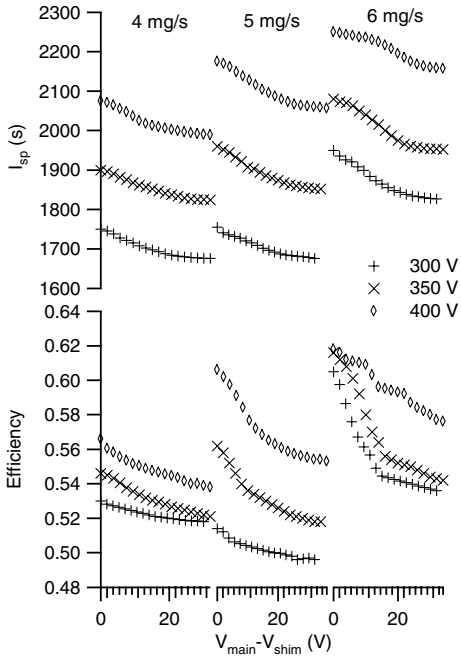

Fig. 6 Efficiency and specific impulse as a function of shim electrode bias voltage. Uncertainty is approximately 5%. Error bars have been omitted for clarity.

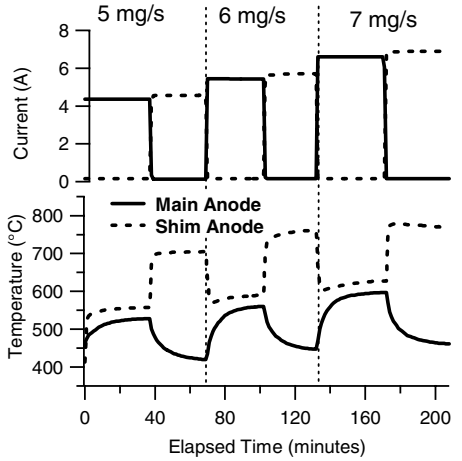

Fig. 7 Thermal response of the segmented-anode Hall thruster with 400 V on the main anode. Temperature uncertainty is approximately 1%.

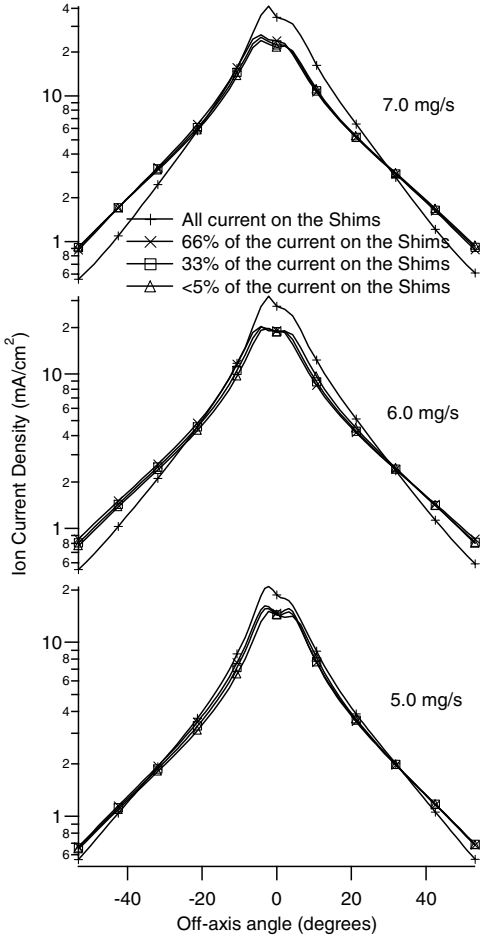

Fig. 8 Ion current density as a function of off-axis angle 250 mm from the thruster with 350 V on the anode. Uncertainty is less than 1%.

stability nor requires significant modifications to the magnetic field, assuming at least 150 mA of discharge current is maintained on the shims at all times. Varying the current attachment requires less than a 10% change in shim electrode voltage and causes a less-than-5% change in specific impulse. No effort was made to optimize the magnetic field as the shim electrode voltage was adjusted. It may be possible to recover the slight efficiency loss seen as the shim electrode voltage was reduced by adjusting the magnetic field at each point either for minimum discharge current or maximum efficiency.

It is interesting to note that there is evidence that the acceleration region is downstream of the shim electrodes. The reduction in shim electrode voltage and subsequent reduction in specific impulse is consistent with the ion velocity loss one would expect by lowering the accelerating voltage. At operating condition 406-1, the specific impulse was 2250 s, which corresponds to an effective accelerating voltage of 332 V. When the shim electrode voltage was lowered to 366 V (to shift current to the main anode) the specific impulse decreased by 93 s to 2157 s corresponding to an effective accelerating voltage of 305 V. And so by reducing the shim electrode voltage by 34 V the effective accelerating voltage was reduced by a comparable 27 V.

B. Thermal Data

In this application, the goal of using segmented anodes was to enable thermal control of the main anode for use in eventual bismuth evaporation. In each of the cases presented in Fig. 4, a 50 + °

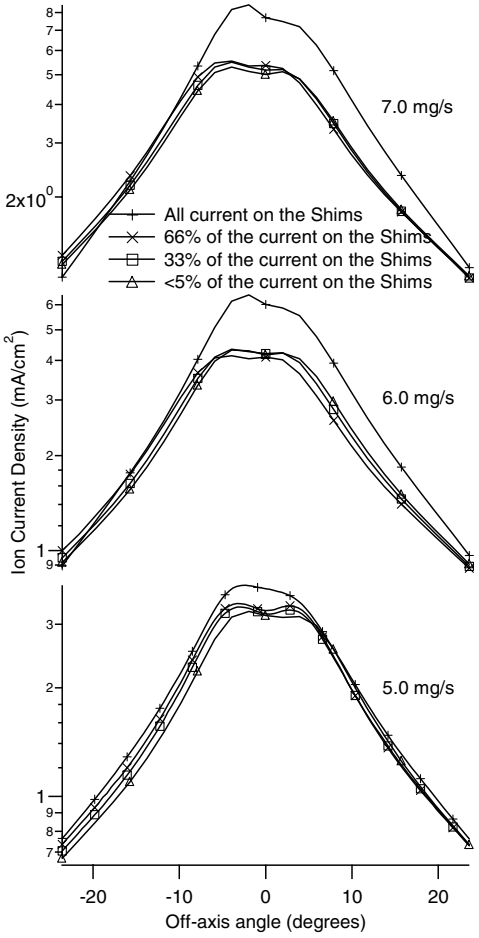

Fig. 9 Ion current density as a function of off-axis angle 500 mm from the thruster with 350 V on the anode. Uncertainty is less than 1%.

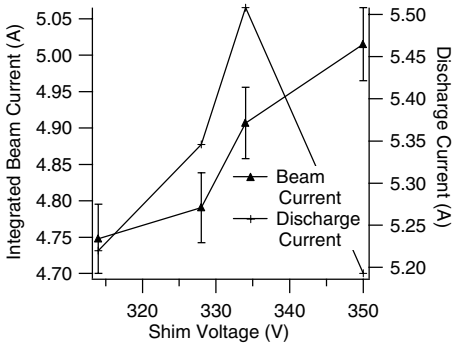

Fig. 10 Integrated beam current and total (shim plus main) discharge current vs shim electrode voltage for the 356 set of operating conditions. Error on the integrated beam current is estimated to be 1%. Error on the measured beam current is less than 1%.

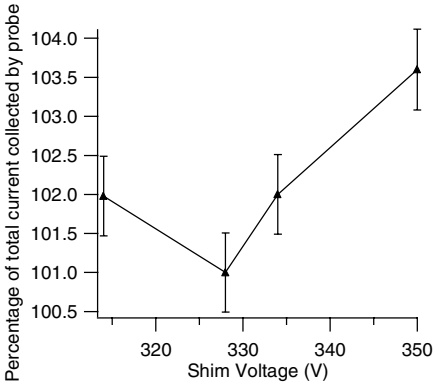

Fig. 11 Percentage of discharge current collected by the Faraday probe as a function of shim electrode voltage for a typical operating condition (350 V, 6 mg/s). Integration error is assumed to be 1%.

variation in temperature was obtained in a matter of minutes for the main anode, and in seconds for the shim electrode. In the thermal region of interest, a 50° swing in temperature would cause a 63% change in the bismuth evaporation rate, providing a wide range of throttleability. Moreover, at the tested power levels, the anodes are both thermally stable and well within the working temperature of the constituent materials. From these results, it is clear that using segmented anodes for thermal control is a valid approach.

Although thermal testing showed the ability to substantially vary the anode temperature, the maximum temperature achieved was well below that required for sufficient bismuth evaporation through self-sustaining operation. It was previously determined [4] that a reservoir temperature of 750°C was required but even running at 2.4 kW the main anode temperature reached a maximum 597°C. To gain the additional 150°, thruster power could be further increased at the expense of thruster lifetime. Another option could be to reduce the anode face area, thereby increasing the power density as well as improving thermal insulation. The thruster employed in this study had a power density of 0.5 W/mm^2 (based on anode face area) and achieved 597°C. Thermal modeling suggests that a power density of 1 W/mm^2 would be sufficient to achieve the goal of 750°C.

C. Probe Data

Integration of the ion current density as a function of off-axis angle provided more insight into the changes in the thruster operating parameters as discharge current was shifted between the main anode and the shim electrodes. Integration was performed on the data taken at 250 mm from the thruster, across the entire angular sweep the probe passed through. The slight beam asymmetry seen was compensated for by integrating over the entire distribution, and not attempting to use one side for the calculation of beam current. The trend in beam current was generally that increasing shim electrode current (by increasing shim voltage) caused total beam current to increase as much as 6%, as shown in Fig. 10.

Comparison of the beam and discharge currents allows determination of whether the increases in beam current were due to higher thruster power or increased beam focusing. Figure 11 shows the percentage of discharge current accounted for by the integrated beam current for a typical operating condition. The fraction of total current collected by the probe varied by as much as 6% between shim electrode sharing levels. The percentage of total current collected by the probe showed a local minimum when the shim voltage was slightly below the main anode voltage.

The changes in beam current due to the adjustment of shim electrode voltage could stem from two factors: change in multiply charged ion fraction or change in propellant use. An increase in multiply charged ions would manifest as an increase in thrust, specific impulse, discharge current, and measured current by the probe. It would also be seen as an efficiency loss. The beam and discharge currents would increase at exactly the same rate, as each multiple ion would produce multiple electrons. This does not appear to be the case. As efficiency and thrust both increased as the shim electrode voltages were increased, it is not probable that the multiply charged ionization fraction is significantly increasing. Whereas a changing multiple-ion fraction cannot be eliminated, the increase in efficiency indicates any change is small. Additionally, as the production of multiply charged ions is a function of the discharge voltage, an increase in multiply charged ions as shim voltage is lowered is counterintuitive; a change in fraction as the shim voltage was changed should produce more multiply charged ions at higher shim voltages, and reverse the trend in efficiency as the shim voltage was adjusted.

The second and more probable cause is that the propellant use is increasing. An increased propellant use fraction would manifest as

increased beam and discharge current, efficiency, and thrust. As each of these requirements is met as shim electrode voltage (and hence, current) is increased, it can be concluded that the thruster becomes more efficient at propellant use as voltage to the shim electrodes approaches that of the main anode. The total propellant use efficiency might also be affected by the nature of the plasma inside the discharge channel; if ionization is taking place at points farther upstream as the current is shifted to the main anode, then ions will have longer required paths to escape the discharge channel, and thus more chances to collide with other particles. This effect cannot be characterized without extensive probe studies inside the discharge channel of the thruster, however.

An interesting phenomenon is that the integrated beam currents were higher in many cases than the theoretical maximum current. The maximum current that should be seen from the integration is determined by assuming 100% propellant use. For the 5.0, 6.0, and 7.0 mg/s mass flow cases, these currents are 3.68, 4.42, and 5.16 A, respectively. The ratios of measured beam current to theoretical beam current ranged between 99% (305 condition set) and over 135% (407 condition set). These values indicate there is a significant source of nonrandom experimental error, resulting in an offset of the collected current values above the theoretical maximum. The most likely cause is collection of charge exchange ions. Previous studies [15] have shown that small currents can be collected in positions outside the thruster plume, an effect attributed to finite facility backpressure during ground testing. Emission of secondary electrons may also be higher than estimated, leading to high ion current measurement. Additional experimentation is necessary to determine if this excess current is the result of a high charge exchange ion density, high secondary electron emission, or other factors.

Overall, the adjustments to shim electrode potential and current seem to have a positive effect on the ion beam as the shim electrode voltage approaches that of the main anode. The increase in peak current density, and in the 356, 357, and 307 operating cases the reduction in off-axis current density, indicate the thruster is more efficiently focusing the ion beam when the shims are accepting most of the discharge current.

VI. Conclusions

A Hall thruster was modified to include segmented anodes, and was tested to determine the effect on the performance of the thruster. Overall, the thruster proved to be more efficient, exhibited higher specific impulse, and had a higher beam current with equal voltages on the shim electrodes and main anode. The beam divergence was slightly affected, with the major differences being a large increase of beam current along thruster centerline and a small decrease in high off-axis angle beam current in some cases, both when the shim electrode voltage was equal to the main anode voltage. The simultaneous increase in thrust, efficiency, specific impulse, and beam current indicate that the thruster was using propellant more efficiently when all current was on the shim electrodes.

Segmenting the anode was shown to be a viable means of obtaining thermal control. Although the ultimate temperatures sought were not obtained, the temperature variation observed lends credibility to the method of direct bismuth evaporation using discharge waste heat. Thermal modeling suggests that increasing the anode power density by reducing face area will be sufficient to achieve the desired 750°C.

References

[1] Kieckhafer, A. W., and King, L. B., "Energetics of Propellant Options for High-Power Hall Thrusters," *Journal of Propulsion and Power*, Vol. 23, No. 1, 2007, p. 21.

[2] Grishin, S., Erofeev, V., Zharinov, A., Naumkin, V., and Safronov, I., "Characteristics of a Two-Stage Ion Accelerator with an Anode Layer," *Zhurnal Prikladnoi Mekhaniki i Tekhnicheskoi Fiziki*, No. 2, March–April 1978, pp. 28–36.

[3] Tverdokhlebov, S. O., Semenkin, A. V., and Polk, J. E., "Bismuth Propellant Option for Very High Power TAL Thruster," AIAA Paper 2002-0348, 2002.

[4] Massey, D. M., "Development of a Vaporizing Liquid Anode for Hall Thrusters," AIAA Paper 2004-3768, 2004.

[5] Massey, D. R., King, L. B., and Makela, J. M., "Progress on the Development of a Direct Evaporation Bismuth Hall Thruster," AIAA Paper 2005-4232, 2005.

[6] Pote, B., and Tedrake, R., International Electric Propulsion Conference Paper 01-35, 2001.

[7] Fisch, N. J., Raitses, Y., Dorf, L. A., and Litvak, A. A., "Variable Operation of Hall Thruster with Multiple Segmented Electrodes," *Journal of Applied Physics*, Vol. 89, No. 4, 2001, p. 2040.

[8] Raitses, Y., Dorf, L. A., Litvak, A. A., and Fisch, N. J., "Plume Reduction in Segmented Electrode Hall Thruster," *Journal of Applied Physics*, Vol. 88, No. 3, 2000, p. 1263.

[9] Diamant, K., Pollard, J., Cohen, R., Raitses, Y., and Fisch, N., "Investigation of a Segmented Electrode Hall Thruster," AIAA Paper 2004-4098, July 2004.

[10] Kieckhafer, A. W., Massey, D. R., King, L. B., and Sommerville, J. S., "Effect of Segmented Electrodes on the Beam Profile of a Hall Thruster," AIAA Paper 2004-4101, July 2004.

[11] King, D., Tilley, D., Aadland, R., Nottingham, K., Smith, R., Roberts, C., Hruby, V., Pote, B., and Monheiser, J., "Development of the BPT Family of U.S.-Designed Hall Current Thrusters for Commercial LEO and GEO Applications," AIAA Paper 1998-3338, 1998.

[12] Haag, T., "Design of a Thrust Stand for High Power Electric Propulsion Devices," AIAA Paper 1989-2829, 1989.

[13] Domonkos, M. T., Marrese, C. M., Haas, J. M., and Gallimore, A. D., "Very Near-Field Plume Investigation of the D55," AIAA Paper 1997-3062, 1997.

[14] Hagstrum, H. D., "Auger Ejection of Electrons from Tungsten by Noble Gas Ions," *Physical Review*, Vol. 96, No. 2, 1954, p. 325.

[15] King, L. B., "Transport-Property and Mass Spectral Measurements in the Plasma Exhaust Plume of a Hall-Effect Space Propulsion System," Ph.D. Dissertation, University of Michigan, 1998.

A. Gallimore
Associate Editor